POLITECNICO DI TORINO
Repository ISTITUZIONALE

Intrinsic electric field effects on few-particle interactions in coupled GaN quantum dots

(Article begins on next page)

22 September 2024

Intrinsic electric field effects on few-particle interactions in coupled GaN quantum dots

S. De Rinaldis,[1,*] I. D'Amico,[2,3] and F. Rossi[2,3,4]

[1]*Chemical Physics Theory Group, Department of Chemistry University of Toronto, 80 St. George Street, Toronto, Ontario, Canada M5S 3H6*

[2]*INFM-Istituto Nazionale per la Fisica della Materia, Italy*

[3]*Institute for Scientific Interchange (ISI), Villa Gualino, Viale Settimio Severo 65, I-10133 Torino, Italy*

[4]*Dipartimento di Fisica, Politecnico di Torino, Corso Duca degli Abruzzi 24, I-10129 Torino, Italy*

We study the multiexciton optical spectrum of vertically coupled GaN/AlN quantum dots with a realistic three-dimensional direct-diagonalization approach for the description of few-particle Coulomb-correlated states. We present a detailed analysis of the fundamental properties of few-particle/exciton interactions peculiar of nitride materials. The giant intrinsic electric fields and the high electron/hole effective masses give rise to different effects compared to GaAs-based quantum dots: intrinsic exciton-exciton coupling, nonmolecular character of coupled dot exciton wave function, strong dependence of the oscillator strength on the dot height, large ground-state energy shift for dots separated by different barriers. Some of these effects make GaN/AlN quantum dots interesting candidates in quantum information processing.

I. INTRODUCTION

In the last few years semiconductor quantum dots (QDs) have been an area of intensive research in condensed matter physics.[1] The possibility of tailoring some of their structural parameters represents a fundamental tool in order to study basic physics and to achieve technological applications.[2–4] The strength of the lateral or vertical coupling between two quantum dots represents a further degree of freedom for engineering optical and electrical properties and for studying few-particle phenomena,[5,6] such coupled nanostructures are also known as "artificial" or "macro" molecules.

The growth of GaN/AlN quantum dots[7] and the demonstration of their vertical and lateral alignment[8] have been recently achieved. While GaAs-based quantum dots have been widely studied both theoretically and experimentally,[9–11] GaN quantum dots are becoming a subject of increasing interest for their potential technological applications, such as quantum information processing,[12] single electron read-out devices[13] or spintronics.[14]

Our analysis is focused on few-particle effects in nitride dots. We address some distinguished few-particle phenomena typical of nitride QDs and mainly stemming from the built-in giant electric field which characterizes such nanostructures. We analyze the behavior of the intrinsic exciton-exciton dipole coupling as a function of the various structure parameters. In addition our calculations show that the ground-state excitonic transition of two identical GaN dots is characterized by a strong blue shift when their relative distance is decreased. The corresponding ground-state excitonic wave function preserves its atomiclike behavior, in contrast to what happens in GaAs-based coupled QDs, where a red shift of the ground state transition and a splitting in bonding and antibonding molecularlike states is observed.[15] We stress that our analysis is also relevant for the experimental realization of the quantum information processing strategy proposed in Ref. 12, in which a large biexcitonic shift is necessary for energy selective addressing of the different few-particle excitations with fs/ps laser pulses.

The paper is organized as follows. In Sec. II we compare the characteristics of GaAs and GaN-based heterostructures, in Sec. III we develop our theoretical approach; in Sec. IV we introduce the investigated system; in Sec. V we focus on exciton-exciton interactions and on the oscillator strength of the transitions. In Sec. VI we study two coupled identical GaN dots and we compare GaAs and GaN macromolecules investigating the role of the different parameters involved. In Sec. VII the main results are summarized and some conclusions are drawn.

II. GaN VERSUS GaAs-BASED QUANTUM DOTS

Let us first of all compare the general characteristics of GaN-based quantum dots with the more familiar GaAs-based ones. The GaAs compounds have a zincblende structure characterized by a face-centered cubic cell. This structure does not present spontaneous polarization, and, in the absence of applied electric fields, the dipole moment of correlated electron-hole excitations will be negligible and so will be the interaction between excitons created in different QDs. For application purposes however, it would be desirable to have a controllable source of interaction between different QDs, since the latter can be naturally thought as the different units of a device. A possibility for creating such an interaction has been envised and studied in Refs. 10 and 11. The underlying idea is to create interacting dipoles, i.e., to separate electron and hole excitonic components by means of an in-plane externally applied (static) electric field.

The great advantage of III-V nitride compounds, as GaN, is that they may present *intrinsic* electric fields, and, as a consequence, they automatically have *built in* such an interaction. III-V nitride compounds may present in fact a wurzite type of structure based on a hexagonal cell, which is compatible with spontaneous bulk polarization, i.e., they present a nonvanishing dipole per unit volume. In the heterostructures we consider, this polarization is accumulated at the

GaN/AlGaN interfaces due to the asymmetry of GaN and AlN unit cells.

In the case of QDs a strong strain-induced piezoelectric field along the (0001) direction must be added to this effect. This is considerably stronger than in GaAs-based nanostructures because the piezoelectric constants in nitrides are orders of magnitude greater than in other III-V compounds. The sum of the two contributions results in a strong built-in electric field of the order of few MV/cm which is oriented along the growth direction, and has opposite sign inside and outside the dot. GaN-based QD are then characterized by strong intrinsic electric fields which automatically creates intrinsic dipoles out of each and every electron-hole correlated pair excitation.

Let us consider two vertically stacked QDs coupled by the exciton-exciton interaction just described. In GaAs the particle distributions corresponding to the biexcitonic ground state generated by laser pulses having the same polarization, will approximately correspond to two parallel dipoles (one for every QD) aligned along the (in-plane) field direction.[11] In this way excitons in two vertically stacked QDs will have a positive Coulomb interaction.

If the corresponding GaN based structure instead, such a state is formed by approximately two dipoles but stacked in the growth direction. Their interaction energy will then be negative. This interaction energy is the so called biexcitonic shift, i.e., the difference in energy between the transition energy corresponding to the creation of a certain exciton and the one corresponding to the same transition but in the presence of another exciton.

In GaAs based structures the biexcitonic shift can be tuned by engineering dots parameters as height and base and by modifying the value of the external applied field. In the case of GaN based the strength of the built in field is instead determined by the structure parameters. In both materials and for experimentally reasonable parameters, it is possible to achieve (at least theoretically) biexcitonic shifts of the order of few meV, which are consistent with fast, subpicosecond, exciton dynamics.

From the previous analysis it is clear that both GaAs and GaN structures may present a tunable exciton-exciton coupling which can be used for different applications and in particular to perform two-qubit conditional operations.[10–12] One drawback of applying an external electric field (as needed in GaAs based structures) is that a too strong electric field might ionize the trapped charges. An externally applied field also means more complex overhead circuits.

Due to the strength of the built-in electric field, the difference in energy between the two lowest excitonic transitions is one order of magnitude bigger in GaN-based structures than the GaAs-based ones. Additionally in the GaN-based structures the oscillator strength associated to ground state excitons in QDs of different heights are different because the QDs height roughly determines the dipole length and this strongly influence electron and hole wave function overlap.

III. THEORETICAL MODEL

The theoretical approach employed to study the optical response of our GaN nanostructure is a fully three-
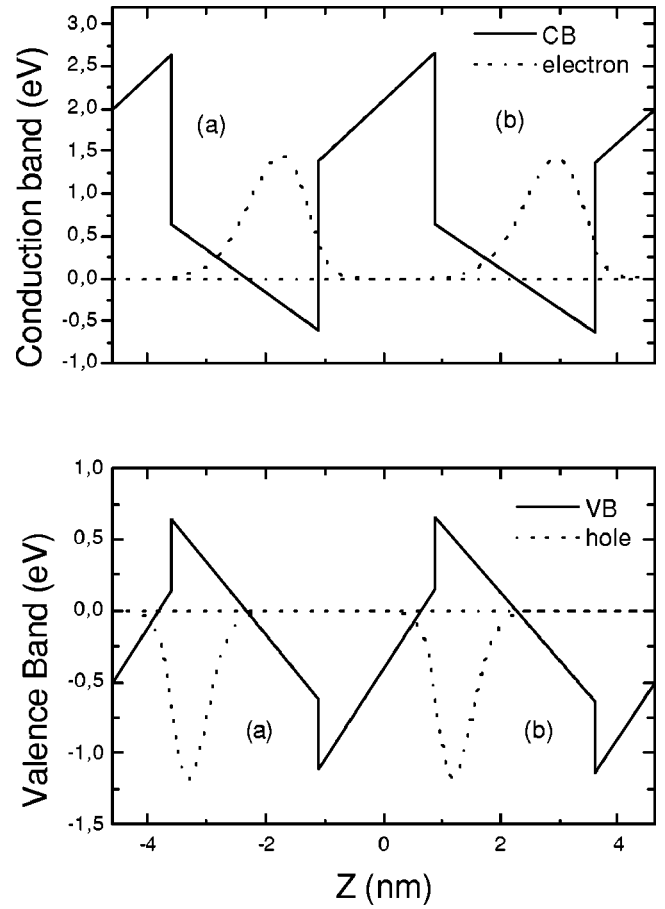

FIG. 1. Electron (upper panel) and hole (lower panel) particle distribution (dotted line), conduction (upper panel) and valence (lower panel) band structure (solid line) along the growth direction for two coupled GaN dots of, respectively, 2.5 nm and 2.7 nm of height, separated by a 2 nm AlN barrier.

dimensional (3D) exact-diagonalization scheme, as described in Ref. 11. The confinement potential of GaN "macromolecule" is modeled as parabolic in the x-y plane and as a sequence of triangularlike potential wells along the growth (z) direction (see Fig. 1).

The physical system under investigation is a gas of electron-hole pairs confined in a semiconductor quantum dot or in two vertically coupled quantum dots. The Hamiltonian is the sum of three terms

$$H = H^c + H^{cc} + H'. \tag{1}$$

The term H^c is a sum of single-particle Hamiltonians which describes a gas of noninteracting carriers, electrons and holes, and includes the QD quasi-zero-dimensional confining potential. The term H^{cc} describes the correlation of the carriers via the two-body Coulomb interaction. The term H' is a light-matter interaction Hamiltonian, which accounts for the laser light absorption in a quantum dot. We consider the multiexciton optical spectra, i.e., the absorption probability corresponding to the generic $N \rightarrow N'$ transition, where N is the exciton number, and, in particular, we evaluate[11] the excitonic ($0 \rightarrow 1$) and biexcitonic ($1 \rightarrow 2$) optical spectra. The

biexcitonic $(1 \rightarrow 2)$ optical spectrum describes the creation of a second electron-hole pair in the presence of a previously generated exciton. Here, we shall consider parallel-spin configurations only. In the following three sections we will describe the three terms of the Hamiltonian.

A. Single-particle description

We will work in the usual effective-mass[18] and envelope-function approximation.[19] Within such approximation scheme, the noninteracting electron and holes wave functions are described by the following Schrodinger equation:

$$-\frac{\hbar^2 \nabla^2}{2m_{e/h}^*} \psi_{e/h} + V^{e/h} \psi_{e/h} = E_{e/h} \psi_{e/h}, \qquad (2)$$

where e/h describes the set of quantum numbers for electrons (e) and holes (h); ψ is the envelope function of the quantum state; $m_{e/h}^*$ is the bulk effective mass for electrons (e) and holes (h); $E_{e/h}$ are the energy levels; $V^{e/h}$ is the three-dimensional confinement potential. Since we are interested only in the lowest energy levels, we can approximate the confinement potential as the sum of two potential profiles acting in the parallel and perpendicular direction to the growth plane. Moreover, a 2D parabolic potential in the x-y plane has been proven to reproduce experimental data.[9] Therefore in our model we consider a 2D parabolic potential, whose analytic solutions are known, and we solve numerically the Schrodinger equation along the growth direction using a plane-wave expansion technique.[20] We expand the unknown envelope function in a plane-wave basis:

$$\psi_{e/h} = \frac{1}{\sqrt{L}} \sum_k b_k e^{ikr}. \qquad (3)$$

We use periodic boundary conditions with a box of length L; $k = n(2\pi/L)$ are the reciprocal lattice vectors. By substituting the plane-wave expansion (3) in the Schrodinger equation (2) we obtain an eigenvalue equation,

$$\sum_k (H_{kk'} - E\delta_{kk'})b_{k'} = 0, \qquad (4)$$

where $H_{kk'}$ are the matrix elements of the single-particle Hamiltonian in a plane-wave basis. A direct diagonalization can be done with standard commercial packages. The electron and hole states expressed in terms of creation/destruction operators are

$$|e\rangle = c_e^\dagger |0\rangle, \qquad (5)$$

$$|h\rangle = d_h^\dagger |0\rangle, \qquad (5)$$

where $|0\rangle$ is the vacuum state. The single-particle Hamiltonian of the system can be rewritten as

$$H^c = H^e + H^h = \sum_e E_e c_e^\dagger c_e + \sum_h E_h d_h^\dagger d_h. \qquad (6)$$

B. Coulomb correlations

The single-particle eigenfunctions and the corresponding eigenvectors are the input for the calculation of Coulomb interactions between the carriers. In writing H^{cc}, we neglect Auger processes that take place only at high particle densities and energy far from the bottom of the band. Only processes conserving the number of carriers are considered:

$$H^{cc} = H^{ee} + H^{hh} + H^{eh}$$

$$= \frac{1}{2} \sum_{e_1 e_2 e_3 e_4} V_{e_1 e_2 e_3 e_4} c_{e_1}^\dagger c_{e_2}^\dagger c_{e_3} c_{e_4}$$

$$+ \frac{1}{2} \sum_{h_1 h_2 h_3 h_4} V_{h_1 h_2 h_3 h_4} d_{h_1}^\dagger d_{h_2}^\dagger d_{h_3} d_{h_4}$$

$$- \sum_{e_1 e_2 h_1 h_2} V_{e_1 e_2 h_1 h_2} c_{e_1}^\dagger d_{h_1}^\dagger d_{h_2} c_{e_2}. \qquad (7)$$

The physical interpretation of the terms in H^{cc} is, respectively, electron-electron and hole-hole repulsive interaction (H^{ee} and H^{hh}) and electron-hole attractive interaction (H^{eh}), while V indicates the Coulomb potential matrix for a generic two-particle transition. After having obtained by direct diagonalization the 3D single-particle electron and hole wave functions, we calculate the matrix elements of the complete many-body Hamiltonian ($H^c + H^{cc}$) in the basis of products of electron and hole eigenstates of the single-particle Hamiltonian. We consider many-body state with the same number of electron and holes, that are in general denoted as exciton $(N=1)$, biexciton $(N=2)$, etc. By direct diagonalization we obtain the energies and wave functions, which will be expressed as a linear combination of products of single-particle states.

C. Matter-light interaction

The light-matter interaction Hamiltonian is

$$H' = -E(t)\left(\sum_{eh} \mu_{eh}^* c_e^\dagger d_h^\dagger + \sum_{eh} \mu_{eh} c_e d_h\right), \qquad (8)$$

where $E(t)$ is the electromagnetic field of the laser and μ_{eh} is the dipole matrix element for the e-h transition that can be factorized as a "bulk" and a wave function dependent part:

$$\mu_{eh} = \mu_{bulk} \int \psi_e^*(r)\psi_h(r)dr. \qquad (9)$$

The matrix elements of the light-matter Hamiltonian are different from zero only for the transitions $N \rightarrow (N+1)$ and $(N+1) \rightarrow N$ that correspond to the absorption and the emission of a photon, respectively (N is the number of electron-hole pairs, that is conserved by $H^c + H^{cc}$). Following the Fermi's golden rule we can calculate the absorption probability for the $N \rightarrow (N+1)$ transition:

$$P(\lambda_N \rightarrow \lambda_{N+1})_E = \frac{2\pi}{\hbar}|H'(\lambda_N \lambda_{N+1})|^2 \delta(E(\lambda_{N+1}) - E(\lambda_N) - E), \qquad (10)$$

where the state $|\lambda_N\rangle$ corresponds to N Coulomb-correlated electron-hole pairs.

TABLE I. Material parameters used in the calculations.

	GaN	GaAs
E_{gap}(eV)	3.5	1.519
m_e^*(m_0 units)	0.2	0.067
m_h^*(m_0 units)	1	0.34
ΔE_c(eV)	2	1
ΔE_v(eV)	0.5	0.3
ϵ(relative)	9.6	12.10

IV. COUPLED GaN DOTS

We study the multiexciton optical response of GaN/AlN QDs in the range of parameters experimentally realized in Ref. 16: the dot height is varied between 2 and 4 nm and the base diameter is varied from 10 to 17 nm, proportionally to the height (according to experimental data in Ref. 16). The material in the dot is assumed to have a constant composition of GaN, while in the barrier is pure AlN, thus neglecting intermixing. The valence-band discontinuity is set, according to experimental values, to 0.5 eV, the conduction band to 2.0 eV.[17] The typical system considered is composed by two QDs stacked along the growth z axis (see Fig. 1); in the in-plane directions the confined potential is assumed to be parabolic. In Table I we compare the different parameters used in this paper for GaN and GaAs quantum dots. GaN has higher electron/hole masses and conduction/valence-band discontinuities. The main feature of wurzite compared to zincoblende GaN heterostructures is the strong built-in electric field. The strength of the intrinsic field is of the same order of magnitude inside and outside the dot (MV/cm), but it is opposite in sign, antiparallel to the growth direction inside the dot. The built-in electric field in GaN QDs and AlN barriers is calculated according to:[21]

$$F_d = \frac{L_{br}(P_{tot}^{br} - P_{tot}^d)}{\epsilon_0(L_d\epsilon_{br} + L_{br}\epsilon_d)}, \qquad (11)$$

where $\epsilon_{br,(d)}$ is the relative dielectric constant of the barrier (of the quantum dot), $P_{tot}^{br,(d)}$ is the total polarization of the barrier (of the quantum dot), and $L_{br,(d)}$ is the width of the barrier (the height of the dot). The value of the field in the barrier F_{br} is obtained by exchanging the indices br and d. Equation (11) is derived for an alternating sequence of quantum wells and barriers, but it is a good approximation also in the case of an array of similar QDs in the growth (z) direction. In our approach the in-plane components of the built-in electric field are in fact "absorbed" in the strongly confining bidimensional parabolic potential which in addition preserves the spherical symmetry of the ground state.[22,23] Our modeling is supported by the agreement with the experimental findings in Ref. 22. The polarization $P_{tot}^{br,(d)}$ is the sum of the spontaneous polarization charge that accumulates at GaN/AlN interfaces and the piezoelectric one, $P_{tot}^{br/d} = P_{piezo}^{br/d} + P_{sp}^{br/d}$. The piezoelectric charge is induced by the lattice mismatch and by the thermal strain ($P_{piezo}^{br/d} = P_{ms}^{br/d} + P_{ts}^{br/d}$). All the material parameters are the ones used in Ref. 21, except

for P_{sp}^{br} and $\sigma_\parallel^{br/d}$ which depend on the aluminum concentration in the barrier: in the quantum wells considered in Ref. 21 such concentration is Al=0.15 while for GaN/AlN quantum dots is Al=1. In particular $\sigma_\parallel^{br/d}=2.48\%$, therefore in GaN-based dots spontaneous polarization and piezoelectric fields have similar values while in $Al_{0.15}Ga_{0.85}N$/GaN quantum well the piezoelectric field contributes only 10% of the total value. The other parameters necessary to calculate the electric field are: $P_{ms}^{br/d}=-2(e_{33}C_{13}/C_{33}-e_{31})\sigma_\parallel^{br/d}$, $P_{ts}^d=-3.2*10^{-4}C/m^2$, $P_{ts}^{br}=0\ C/m^2$, $P_{sp}^{br}=-0.081\ C/m^2$, and $P_{sp}^d=-0.029\ C/m^2$.

The giant internal field strongly modifies the conduction and valence bands along the growth direction and causes the separation of electrons and holes, driving the first one toward the QD top and the latter toward its bottom. This corresponds to the creation of intrinsic dipoles. In this context, the charge distribution of two vertically coupled GaN dots occupied by one exciton each can be described as two dipoles aligned along the growth direction. This is exemplified in Fig. 1, where we plot the electron and hole single-particle distributions corresponding to the lowest biexcitonic state (with parallel-spin excitons) for one of the GaN/AlN quantum dot nanostructure considered. Nearby quantum dots are then coupled by the corresponding exciton-exciton (dipole-dipole) interaction.

V. BIEXCITONIC SHIFT AND OSCILLATOR STRENGTH

The energy renormalization of the excitonic transition in the presence of another exciton is known as biexcitonic shift. A biexcitonic shift of the order of few meV in two coupled GaN dots is the prerequisite for the implementation of conditional quantum dynamics in the quantum information/computation scheme proposed in Ref. 12. In the aforementioned scheme excitons in different QDs are manipulated by energy-selective addressing; additionally, due to the strain field, two stacked QDs are in general not identical, therefore we set the difference between the well widths of two stacked QDs to be 8%.[24] This allows for energy-selective generation of ground-state excitons in neighboring QDs. For the range of parameters considered, the barrier width is such to prevent single-particle tunneling and to allow at the same time significant dipole-dipole Coulomb coupling. In contrast to GaAs quantum dots, even with a 2 nm barrier the single-particle tunneling is negligible on the nanosecond time scale (i.e., on a time scale comparable to the excitonic lifetime). This is due to the higher valence/conduction band gaps and electron/hole effective masses.

The theoretical approach employed to study the optical response of our GaN nanostructure is a fully three-dimensional exact-diagonalization scheme, as described in Sec. III. The confinement potential of GaN macromolecule is modeled as parabolic in the x-y plane and as a sequence of triangularlike potential wells along the growth (z) direction (see Fig. 1). We evaluate the excitonic ($0 \rightarrow 1$) and biexcitonic ($1 \rightarrow 2$) optical spectra. The biexcitonic ($1 \rightarrow 2$) optical spectrum describes the creation of a second electron-hole pair in the presence of a previously generated exciton. Here, we shall consider parallel-spin configurations only. For all
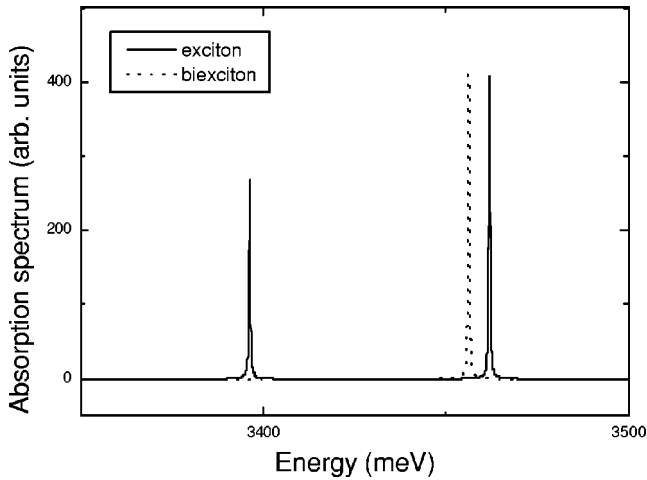
FIG. 2. Excitonic (solid line) and biexcitonic (dashed line) absorption spectrum of the GaN coupled dots of Fig. 1.
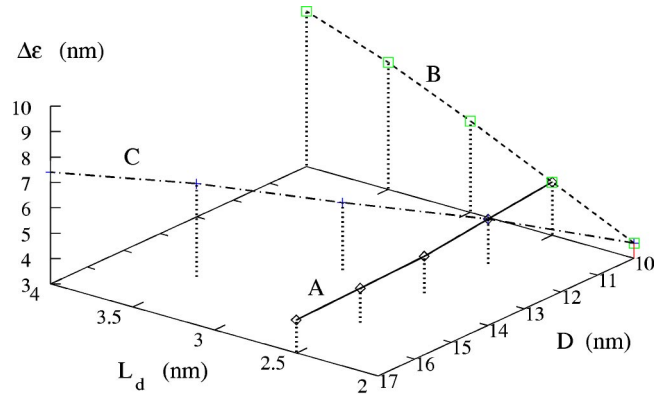

FIG. 3. Biexcitonic shift of the ground-state transition in dot b for two coupled GaN dots as a function of dot height and base diameter. In curve (A) only the base diameter of the dots is changed ($D=10$ nm); in curve (B) only the height of the dots is changed ($L_d=2.5$ nm), while in curve (C) D is varied proportionally to L_d. The parameters for the parabolic potential is varied in the range: $\hbar\omega_e=74-290$ meV, $\hbar\omega_h=33-130$ meV. In particular, the values analyzed in the figures are $D=10$ nm ($\hbar\omega_e=290$ meV, $\hbar\omega_h =130$ meV), $D=11.75$ nm($\hbar\omega_e=170$ meV, $\hbar\omega_h=76$ meV), $D =13.5$ nm($\hbar\omega_e=131$ meV, $\hbar\omega_h=59$ meV), $D=15.25$ nm($\hbar\omega_e =97$ meV, $\hbar\omega_h=43$ meV), $D=17$ nm($\hbar\omega_e=74$ meV, $\hbar\omega_h =33$ meV).

the structures considered, the two lowest optical transitions are, respectively, direct ground-state excitons in dot a and b (see Fig. 1). In Fig. 2 we show an example of such an absorption spectrum for the parameters of Fig. 1. In such example a negative exciton-exciton coupling $\Delta\epsilon=5.7$ meV is the signature of the creation of vertically aligned dipoles forming the biexcitonic ground state.

Let us focus on the biexcitonic shift defined in the present case as the energy difference between the ground-state biexcitonic transition (given a ground-state exciton in dot a) and the ground-state excitonic transition of dot b. This quantity provides the essential coupling for realizing conditional gates in exciton-based all-optical quantum information schemes.[10,12].

The biexcitonic shift can be engineered by varying the coupled GaN dots parameters with self-assembled growth. We analyze how it depends on the height and base diameter of the dot and barrier between the dots. We also study the corresponding variation of the oscillator strength of the transition. Figure 3 shows how the biexcitonic shift depends on the dimensions (height L_d and base diameter D) of the dot, for a barrier width that is equal to 2.5 nm. We have considered three cross sections of the space parameters, the first (solid line, A) keeping the QD height fixed ($L_d=2.5$ nm), the second (dashed line, B) fixing the base diameter to $D =10$ nm (small dots), and the third (dashed-dot line, C) varying the base diameter proportionally to the height, according to the experimental relation $D=3.5L_d+3$ nm.[16] The height and base diameter values plotted corresponds to the smaller dot.

The excitonic dipole length is roughly proportional to the height of the dot because of the MV/cm built-in electric field; therefore the dependence of the exciton-exciton interaction on the QD height is the strongest (curve B).

By looking at curve A, instead, we notice that the spreading of the wave function related to a wider dot basis, negatively affects the biexcitonic shift: in fact this decreases from 5.1 to 4.3 meV, as the base diameter goes from 10 to 17 nm.[16] Exciton-exciton interaction is favored by "localized" states, virtually achieving a maximum in an idealized "pointlike" particle case.

Curve C presents the experimentally most common case in which base and height of the dots change simultaneously. For realistic parameters the biexcitonic shift can be up to 20% smaller than in curve B, where the wave function is more localized, being the diameter fixed to the value of the "small" dots. In such case it is possible to achieve biexcitonic shifts up to 9.1 meV.

Our results show that the best strategy to achieve large biexcitonic shift is to grow "high" and "small diameter" dots. Unfortunately the oscillator strength (OS) of the ground-state transition strongly decreases with the height of the dot, since it is proportional to the overlap of electron and hole wave functions. Since the coupling of the laser field to the considered transition is directly proportional to this quantity, in view of an all-optical manipulation of correlated electron-hole pair excitations, it is of utmost importance to study the dependence of the OS on the various parameters. In Fig. 4 the OS corresponding to the excitonic ground state of dot b is plotted for the same parameters of Fig. 3 (same labeling of the curves). Curve B (fixed base) shows that the OS decreases superexponentially with the height of the dot. It changes over three order of magnitude from 2 nm to 4 nm height dot. It is interesting to notice that, on the other hand, the width of the dot does not influence the electron-hole overlap, so curve A (fixed L_d) is practically a constant over the whole D range and the two curves B and C corresponding to different diameters, coincide.[25]

In the range of height values considered in Fig. 3, the OS varies over three orders of magnitude, so care must be taken in a future quantum information processing experiment in order to optimize at the same time biexcitonic shift and OS.[26]

Let us now examine the influence of the barrier on the biexcitonic shift and oscillator strength. In Fig. 5 we show
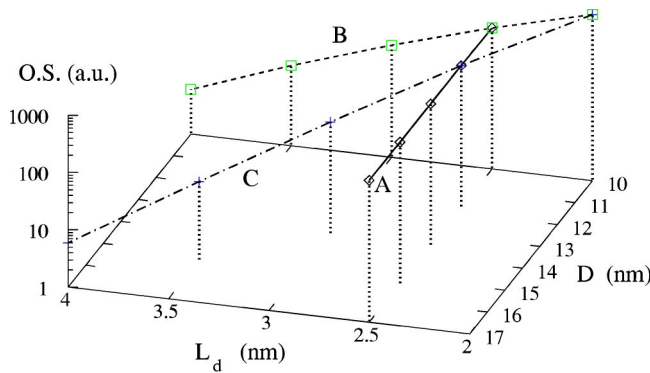
FIG. 4. Oscillator strength of the ground-state transition in dot *b* for the same parameters of Fig. 3; labeling as in Fig. 3.

FIG. 6. Excitonic distribution in a 2.5 nm dot of a coupled dot nanostructure when the barrier width is 2 nm (solid line) and 10 nm (dotted line).

(upper panel, curve *A*) the decreasing of the biexcitonic shift with the barrier width for two coupled dots of 2.5 nm and 2.7 nm of height. We notice that it deviates from a dipole-dipole interaction behavior (curve *B*) and it is 0, 5 meV even at 10 nm barrier. The reason for this behavior can be inferred from Eq. (1). The electric field in the dot increases with the barrier width, and, as a consequence, also the dipole length. The two competing effects result in a slower decreasing of the biexcitonic shift with the barrier. Curve *B* corresponds to the pointlike approximation, for a fixed dipole length (about 1.5 nm) corresponding to a 2 nm barrier. We see that the pointlike biexcitonic shift is two times bigger when the bar-
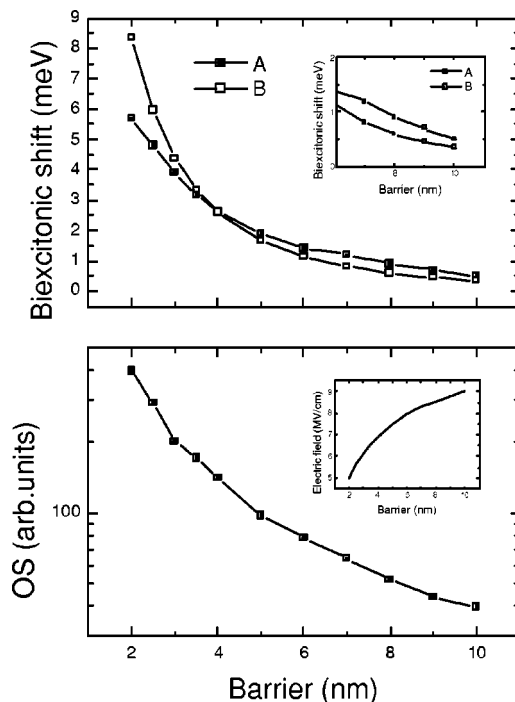
rier is 2 nm, there is a crossover at 4 nm, after which it remains smaller than the exact result. The most striking consequence of the *barrier-dependent* built-in electric field, is that the oscillator strength strongly varies too (lower panel), even if the dimensions of the two dots are kept fixed. In addition (and in contrast to Figs. 3 and 4), in this case *both* OS and biexcitonic shift are *increased* by a smaller barrier, suggesting that the best structure for optical excitonic manipulations and energy-selective addressing techniques is characterized by small interdot barriers. In this respect it would be very interesting to have experimental confirmation of our prediction.

In Fig. 6 we plot the direct comparison of electron and hole distributions of the 2.7 nm dot, for two different barrier width (2 nm and 10 nm). The width of the barrier changes the internal electric field in the dot, that in turns strongly modifies the wavefunctions. The dipole length changes of about 30% (Fig. 6), going from about 1.5 nm at 2 nm barrier, to 1.9 nm when the barrier is 10 nm wide.

Compared to GaAs quantum dots, nitride dots have higher effective masses $m_{e,h}^*$ of both electrons and holes, lower dielectric constant and higher (about two times) conduction and valence band discontinuities $V_{e,h}$. As a consequence, the GaN bulk excitonic Bohr radius is about four times smaller than the GaAs one and the distributions of confined particles are more localized, because their wavelength penetration $L_{e,h}$, where $L_{e,h} = \hbar / \sqrt{2m_{e,h}V_{e,h}}$, depends on such parameters.

The reduction of these two characteristic lengths causes a faster decrease of the electron-hole overlap, as a function of the dipole length and consequently a stronger sensitivity of the oscillator strength (roughly proportional to the electron-hole overlap in the strong confinement regime we are considering) to quantities such as the height of the dot (Fig. 4) or the different built-in electric field (Fig. 5), which strongly affect the dipole length.

Our results demonstrate that there exist a wide range of parameters for which the biexcitonic shift of the order of meV. This is a central prerequisite for realizing energy-

FIG. 5. Upper panel: curve (*A*) shows the biexcitonic shift of the ground state transition in dot *b* for two coupled GaN dots of 2.5 and 2.7 nm of height vs barrier width between the dots. Curve (*B*) shows the corresponding biexcitonic shift in the pointlike charge approximation. Inset: as in main panel, but for large barrier widths. Lower panel: oscillator strength for the same parameters described above. Inset: internal electric field in dot b vs barrier width.
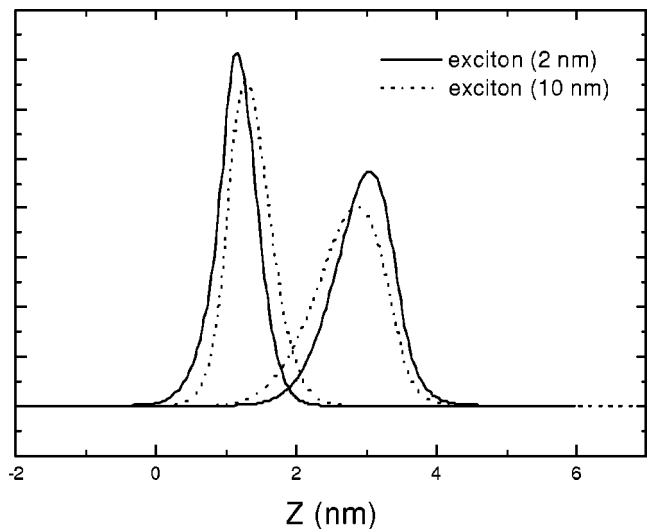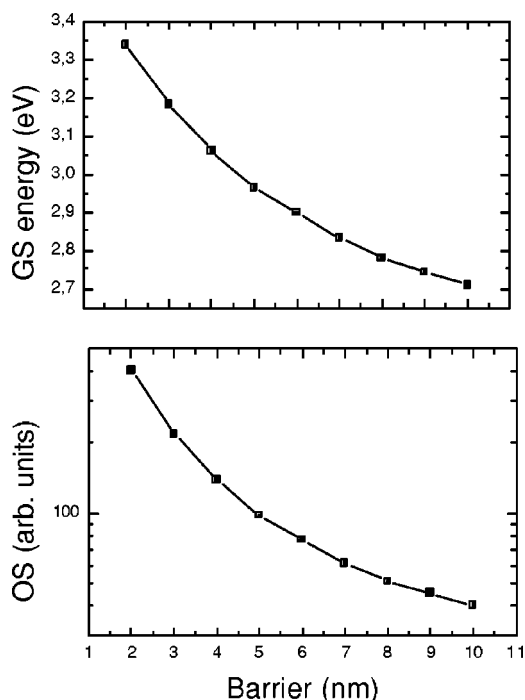
FIG. 7. Exciton ground-state energy (upper panel) and oscillator strength (lower panel) in the dot b of two identical coupled GaN dots of 2.5 nm of height vs barrier between the dots.

selective addressing with subpicosecond laser pulses, as requested, for example, by all-optical quantum information processing schemes[10,12] or read-out devices.[13]

VI. BLUE SHIFT AND ABSENCE OF MOLECULAR STATES

Another interesting effect peculiar of hexagonal GaN/AlN quantum dot is the blue shift of the ground-state transition when the distance between the dots is decreased, without the lifting of the degeneracy of bonding-antibonding states. In GaAs-based quantum dots[28,29] there is a red shift and an increasing energy difference between bonding and antibonding states, which are spread over the whole macromolecule for both electron and hole; on the contrary in GaN QDs, over the range of parameters here considered, the lowest states preserve their atomiclike shape. This depends on the fact that both electron and hole effective masses and valence-conduction-band discontinuities are much larger than in GaAs, therefore *decreasing* the atomiclike wave function overlap responsible for the molecular bonding. However, as discussed in the preceding section, the built-in electric field is not only a function of the dot parameters, but it depends strongly on the barrier width. In particular it increases when the barrier is increased, to saturate at the value $F_d \sim (P_{tot}^{br} - P_{tot}^d)/(\epsilon_0 \epsilon_d)$, corresponding to an isolated dot. For examples it increases from 5 MV/cm for a 2 nm barrier to 9 MV/cm for a 10 nm barrier for the dot parameters of Fig. 6 (see inset). In Fig. 7 we consider two *identical* dots separated by increasing barrier width. As a consequence of the electric-field change, the ground-state energy changes of

more than 600 meV, from 3337.5 meV to 2709.5 meV (upper panel of Fig. 7). Also the oscillator strength is modified (lower panel of Fig. 7) of one order of magnitude, decreasing very fast up to 5 nm barrier width, showing a slower decreasing afterward. In the particular case of *exactly* identical quantum dots, because of the symmetry of the system, the single exciton eigenstates are $|\psi_a\rangle = \frac{1}{\sqrt{2}}(|01\rangle + |10\rangle)$ and $|\psi_b\rangle = \frac{1}{\sqrt{2}}(|01\rangle - |10\rangle)$ and the energy splitting is given by $2V_F$ where V_F is the Foerster energy.[30] V_F is proportional to the square of electron-hole overlap,[30] therefore is much lower in GaN than in GaAs. For example the maximum value for the parameter considered in this work, corresponding to 2 nm dot's height and 2 nm barrier, is only 0.05–0.06 meV. However we stress that when the dots are slightly different, this effect rapidly vanishes since it depends on the ratio $(V_F/\Delta)^2$ where Δ is the energy difference between the two levels coupled by the Foerster transfer process. In GaN dots, differently form GaAs, with an 8% difference in size, Δ is already of the order of hundreds of meV, causing this effect to be extremely difficult (if not impossible) to be observed experimentally.

To qualitatively investigate the effects of the different parameters involved we have calculated the ground state electron and hole distribution for some GaAs-GaN "mixed case," i.e., some artificially designed molecules with one GaN parameter (electric field, valence-conduction band offsets, effective masses) substituted by the corresponding GaAs one. We will consider a nanostructure composed by two dots of 2.5 nm and 2.7 nm separated by a 2 nm barrier. As a benchmark we also plot the "pure GaAs" case [Fig. 8(b)]: its ground state has both hole and electron distributions delocalized over the macromolecule, forming bonding molecular states. The corresponding "pure GaN" case is plotted in Fig. 1 and it is characterized by electron and hole distributions localized in a single dot. The coupled GaN dots without the giant electric field [Fig. 8(d)] still present an atomic character. The same holds for an artificial GaN macromolecule with GaAs effective masses [Fig. 8(c)], and an artificial GaN nanostructure with GaAs conduction/valence band structure [Fig. 8(a)]. It is interesting to note that the electron and hole distribution of a GaN dots without electric field [Fig. 8(d)] are more extended than when a giant electric field is present (Fig. 1). We conclude that the single dot confinement of the excitonic wave function in GaN QDs is a robust feature and that all the parameters involved are responsible for the absence of molecularlike states in GaN coupled dots.

VII. SUMMARY AND CONCLUSIONS

We have performed a detailed investigation of the optical spectrum of coupled GaN quantum dots. In particular, we have shown some effects peculiar to wurzite nitride materials compared to GaAs-based nanostructures: the absence of ground-state exciton wave function delocalization even for relatively short barriers (up to 2 nm) due to the large effective mass/band offsets of nitrides; the presence of a large exciton-exciton interaction between neighbor quantum dots, caused by the giant intrinsic electric fields. We have also
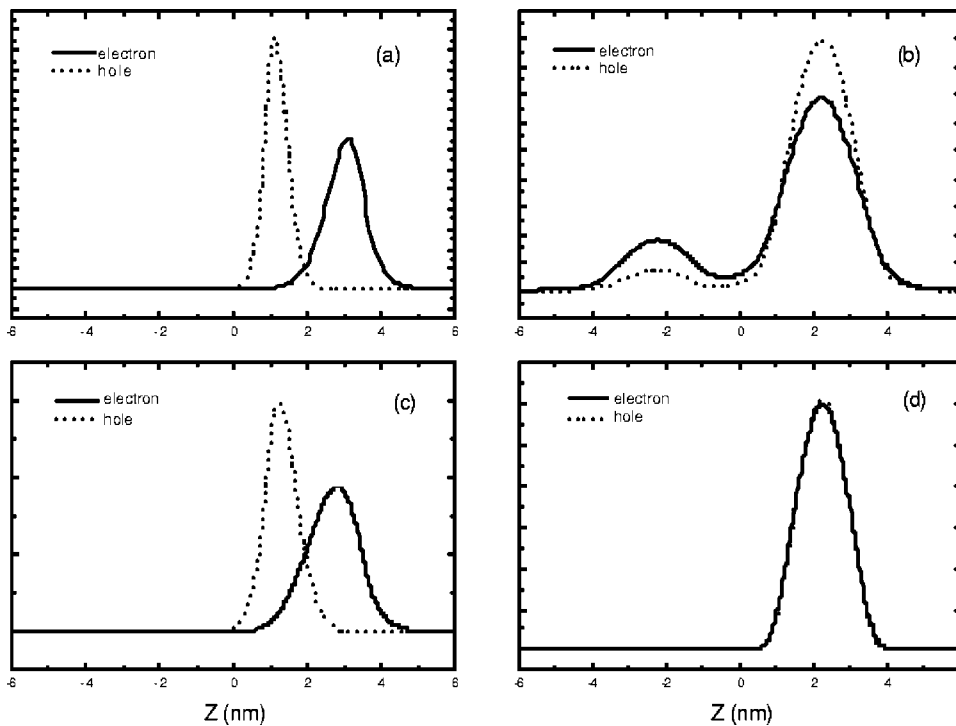
FIG. 8. Electron and hole particle distribution along the growth direction for two coupled dots of, respectively, 2.5 nm and 2.7 nm of height, separated by a 2.5 nm AlN barrier. The dot parameter sets corresponds to: (a) GaN, except valence/conduction band offset (GaAs one); (b) GaAs; (c) GaN, except electron/hole masses (GaAs ones); (d) GaN, except that the electric field is set to zero.

shown that a shift of energy levels of identical quantum dots is expected when the distance between them is varied: such blue shift *is not caused by molecular coupling of the wave function*, but by the decreasing of the built in electric field as the interdot barrier decreases. We have also shown how it is possible to engineer the interdot biexcitonic shift and the corresponding oscillator strength by varying the structural parameters (base, height, barrier) of the dots. Such analysis is crucial in the mainframe of quantum information processing schemes[12] and in general for all-optical devices based on energy-selective addressing[13] in which the conditional excitonic dynamics is based on such quantity.

*Electronic address: srinaldi@chem.utoronto.ca

[1] See, e.g., L. Jacak, P. Hawrylak, and A. Wojs, *Quantum Dots* (Springer, Berlin, 1998); D. Bimberg, M. Grundmann, and N. N. Ledentsov, *Quantum Dot Heterostructures* (Wiley, Chichester, 1998) and references therein.

[2] H. Saito, K. Nishi, and S. Sigou, Appl. Phys. Lett. **78**, 267 (2001).

[3] J. J. Finley, M. Skalitz, M. Arzberger, A. Zrenner, G. Bohm, and G. Abstreiter, Appl. Phys. Lett. **73**, 2618 (1998); G. Yusa and H. Sakaki, *ibid.* **70**, 345 (1997); T. Lundstrom, W. Schoenfeld, H. Lee, and P. M. Petroff, Science **281**, 2312 (1999).

[4] M. Bruchez, Jr., M. Moronne, P. Gin, S. Weiss, and A. P. Alivisatos, Science **281**, 2013 (1998).

[5] G. Ortner, M. Bayer, A. Larionov, V. B. Timofeev, A. Forchel, Y. B. Lyanda-Geller, T. L. Reinecke, P. Hawrylak, S. Fafard, and Z. Wasilewski, Phys. Rev. Lett. **90**, 086404 (2003).

[6] I. Shtrichman, C. Metzner, B. D. Gerardot, W. V. Schoenfeld, and P. M. Petroff, Phys. Rev. B **65**, 081303 (2002).

[7] M. Miyamura, K. Tachibana, and Y. Arakawa, Appl. Phys. Lett. **80**, 3937 (2002); K. Tachibana, T. Someya, S. Ishida, and Y. Arakawa, J. Cryst. Growth **237-239**, 1312 (2002).

[8] J. Brault, S. Tanaka, E. Sarigiannidou, J.-L. Rouviere, B. Daudin, G. Feuillet, and H. Nakagawa, J. Appl. Phys. **93**, 3108 (2003).

[9] R. Rinaldi, S. Antonaci, M. De Vittorio, R. Cingolani, U. Hohenester, E. Molinari, H. Lipsanen, and J. Tulkki, Phys. Rev. B

62, 1592 (2000); I. D'Amico and F. Rossi, Appl. Phys. Lett. **79**, 1676 (2001).

[10] E. Biolatti, R. C. Iotti, P. Zanardi, and F. Rossi, Phys. Rev. Lett. **85**, 5647 (2000).

[11] E. Biolatti, I. D'Amico, P. Zanardi, and F. Rossi, Phys. Rev. B **65**, 075306 (2002).

[12] S. De Rinaldis, I. D'Amico, E. Biolatti, R. Rinaldi, R. Cingolani, and F. Rossi, Phys. Rev. B **65**, R081309 (2002).

[13] I. D'Amico and F. Rossi, Appl. Phys. Lett. **81**, 5213 (2002).

[14] B. Beschoten, E. Johnston-Halperin, D. K. Young, M. Poggio, J. E. Grimaldi, S. Keller, S. P. DenBaars, U. K. Mishra, E. L. Hu, and D. D. Awschalom, Phys. Rev. B **63**, R121202 (2001).

[15] S. Fafard, M. Spanner, J. P. McCaffrey, and Z. R. Wasilewski, Appl. Phys. Lett. **76**, 2268 (2000); G. Schedelbeck, W. Wegscheider, M. Bichler, and G. Abstreiter, Science **278**, 1792 (1997); M. Bayer, P. Hawrylak, K. Hinzer, S. Fafard, M. Korkusinski, Z. R. Wasilewski, O. Stern, and A. Forchel, *ibid.* **291**, 451 (2001).

[16] M. Arley, J. L. Rouviere, F. Widmann, B. Daudin, G. Feuillet, and H. Mariette, Appl. Phys. Lett. **74**, 3287 (1999); F. Widmann, B. Daudin, G. Feuillet, Y. Samson, J. L. Rouviere, and N. Pelekanos, J. Appl. Phys. **83**, 7618 (1998).

[17] S. W. King, C. Ronning, R. F. Davis, M. C. Benjamin, and R. J. Nemanich, J. Appl. Phys. **84**, 2086 (1998).

[18] See, e.g., P. Y. Yu and M. Cardona, *Fundamentals of Semiconductors* (Springer-Verlag, Berlin, 1996).

[19] See, e.g., G. Bastard, *Wave Mechanics Applied to Semiconductor Heterostructures*, Les Editions de Physique (Les Ulis, France, 1988).

[20] F. Rossi and E. Molinari, Phys. Rev. Lett. **76**, 3642 (1996); Phys. Rev. B **53**, 16 462 (1996).

[21] R. Cingolani, A. Botchkarev, H. Tang, H. Morkoc, G. Traetta, G. Coli', M. Lomascolo, A. Di Carlo, F. Della Sala, and P. Lugli, Phys. Rev. B **61**, 2711 (2000).

[22] R. D. Andreev and E. O. O'Reilly, Phys. Rev. B **62**, 15851 (2000); F. Widmann, J. Simon, B. Daudin, G. Feuillet, J. L. Rouviere, N. T. Pelekanos, and G. Fishman, *ibid.* **58**, R15989 (1998).

[23] T. Bretagnon, S. Kalliakos, P. Lefebvre, P. Valvin, B. Gil, N. Grandjean, A. Dussaigne, B. Damilano, and J. Massies, Phys. Rev. B **68**, 205301 (2003).

[24] Q. Xie, A. Madhukar, P. Chen, and N. P. Kobayashi, Phys. Rev. Lett. **75**, 2542 (1995); J. Tersoff, C. Teichert, and M. G. Lagally, *ibid.* **76**, 1675 (1996).

[25] This is not a general fact, but it comes from the constant ratio between bottom base diameter and top base diameter assumed in the model, according to experimental data (Ref. 16). This in turn causes a constant ratio between the width of electron and hole wave functions and therefore a constant oscillator strength when only the base diameter is changed.

[26] A figure of merit, which allows to optimize the interplay between biexcitonic shift and oscillator strength, was introduced in Ref. 27.

[27] S. De Rinaldis, I. D'Amico, and F. Rossi, Appl. Phys. Lett. **81**, 4236 (2002).

[28] M. Arley, J. L. Rouviere, F. Widmann, B. Daudin, G. Feuillet, and H. Mariette, Appl. Phys. Lett. **74**, 3287 (1999).

[29] F. Troiani, U. Hohenester, and E. Molinari, Phys. Rev. B **65**, R161301 (2002).

[30] B. W. Lovett, J. H. Reina, A. Nazir, B. Kothari, and G. A. D. Briggs, Phys. Lett. A **315**, 136 (2003); B. W. Lovett, J. H. Reina, A. Nazir, and G. A. D. Briggs, Phys. Rev. B **68** 205319 (2003).